Pharmaceutical Research, Vol. 7, No. 11, 1990

Research Article

Characterization of a Hot-Melt Fluid Bed Coating Process for Fine Granules

Michael J. Jozwiakowski,[1,2] David M. Jones,[3] and Robert M. Franz[1]

Received November 21, 1989; accepted May 11, 1990

The equipment modifications and process changes necessary to perform hot-melt particle coating in a fluid bed granulator are reviewed. A specific case is presented in which partially hydrogenated cottonseed oil is coated onto fine granules (mean particle size, 77 μm; range, 10–150 μm; one standard deviation is 10 μm) composed of a hydrophobic drug and sucrose. The major variables were product bed temperature, temperature of the wax, spray rate, and atomization air pressure. The product bed temperature was selected to give the optimum congealing rate, and the latter three variables were varied in a statistically designed experiment. The physical properties of wax-coated granules fabricated using combinations of process variables were examined. Response surface analysis was used to determine the optimum process settings in terms of dissolution, particle size, and density of the coated product. This system proved quite adequate for the production of uniformly coated granules, with the best product being obtained at the optimized conditions using 120°C atomization air and molten coating temperature, 30 g/min as the spray rate, and an atomization air pressure of 5 bar.

KEY WORDS: hot-melt coating; microencapsulation; cottonseed oil; optimization; wax coating.

INTRODUCTION

Wax Microencapsulation

The technique of applying hot-melt coatings onto a fluidized bed of particles has received no appreciable attention in the pharmaceutical literature. A number of researchers have reported on the effect of wax coatings generated by spray-congealing of drug/molten wax slurries (1–4), solvent evaporation (5–8), or chilling melts in stirred vessels (9,10) on formulation properties. The *in vitro* release rates for formulations spray-congealed from slurries were affected by the type of wax (2,4), the type of nozzle (2), and the addition of surfactants (2,3). Wax coating affected the flow properties of lactose (7) and the strength of tablets made from these powders (8). While wax-coated formulations are poorly wettable in aqueous media (8), they may enhance bioavailability *in vivo* by reducing the degradation of acid-labile compounds (5) or prolonging the duration of action (9,10). In the present paper we describe the effect of fluidized bed wax coating on the physical properties of fine particles (<150 μm) and the differences caused by varying the coating parameters.

Hot-Melt Coating

Employed for many years for drying and granulating, the standard fluidized bed (Fig. 1, left) has successfully been used for coating small pellets, granules, and particles using molten materials. The product container is an unbaffled, inverted, and truncated cone with a fine retention screen and, in some circumstances, a permeable filter cloth at its base. Using a high air velocity, the substrate is accelerated past the nozzle, which sprays the coating liquid countercurrently into the randomly fluidized bed. The coated particles travel through this "zone" into the larger-diameter expansion chamber, where they cool slightly and decrease in velocity. When their velocity drops to zero, they fall back into the product container and continue cycling throughout the duration of the process. The openness of the product container results in no resistance to particle flow, which is essential for adequate fluidization.

Materials with a melting point of less than 80°C can be applied by carefully controlling the spray liquid atomizing air temperature and the product temperature. The coating is maintained at a constant temperature, usually 40–60°C above its melting point. It is applied using a binary nozzle; liquid is supplied at low pressure and is atomized into droplets by pressurized air. To keep the particles small and discrete, a high atomization air pressure (4–6 bar) is employed. At such high pressures, the air velocity is extreme and may result in pulverization of fragile substrates. Small droplet size is also achieved by the typically low viscosity of the melt and the relatively slow spray rate. The nozzle wand is coaxial with the atomization air, completely surrounding the liquid line to the nozzle port tip. The atomization air is heated to the same temperature as the spray liquid and serves to keep the molten coating at its application temperature. The nozzle wand must be insulated to prevent remelting of coated particles which contact it during fluidization. It is positioned as low as

[1] Pharmaceutics Department, Glaxo Inc., Research Triangle Park, North Carolina 27709.
[2] To whom correspondence should be addressed.
[3] Glatt Air Techniques, Inc., Ramsey, New Jersey 07446.

0724-8741/90/1100-1119$06.00/0

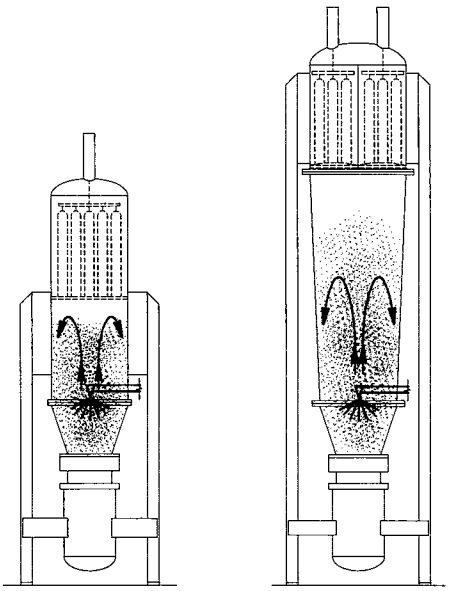

Fig. 1. Comparison of standard fluid bed granulator (left) and one designed especially for particle coating (right) which facilitates hot-melt coating. Major revisions include the lengthened expansion chamber, the conical shape of the expansion chamber, and the provision for alternate filter shaking without interrupting fluidization.

possible in the expansion chamber to minimize the distance that the droplets travel before impinging on a substrate particle. In this manner, premature spray congealing is inhibited.

The quality of the coating is dependent on the congealing rate and the application rate. At lower product temperatures, the coat contains more pores and defects due to congealing prior to complete spreading. Product temperatures too close to the melting temperature of the coating result in wet, sticky beds that may favor particle–particle agglomeration. As the product temperature (controlled primarily by the fluidization air temperature) approaches the melting point of the coating, the bed becomes viscous. The liquid spray rate is slow in comparison to that used when applying coating solutions or dispersions; however, since it is not diluted, the rate of solids application is high. A 20% weight/weight coating can be applied in 1 hr or less. Within a range, slower spray rates lead to a more uniform distribution of the coating material. Slower spray rates inhibit agglomeration by allowing adequate cooling prior to application of subsequent layers, keeping the bed drier.

While it is possible to conduct hot-melt coating in the standard fluid bed granulators, newer fluid beds designed specifically for powder coating facilitate these techniques (Fig. 1, right). These coaters incorporate a lengthened conical expansion chamber and a split filter housing which returns fines (by shaking) to the batch without interrupting fluidization. These two improvements allow a faster liquid application rate (due to higher particle velocities) and operation at a slightly elevated product temperature, resulting in better coat quality. With some of the older granulators which do not have split filter housings that alternate sides during shaking or engage blow-back filter systems, during filter shaking the bed is at rest, and the layer in contact with the bottom screen may locally superheat and melt. As the screen becomes occluded, the fluidization air volume will decrease (as will particle velocity), and agglomeration will occur. Since fluidization in the newer designs is continuous, product contact with the bottom screen is only momentary.

Hot-melt coating can be accomplished in machines with product containers ranging in size from 10 to 1560 liters. A single-headed nozzle is used in machines up to 220 liters, and a three- or six-headed nozzle is used in a production scale coater. In some applications, multiple nozzle systems have been used. Although fluid bed machines smaller than 10 liters are available, their use is discouraged because it is difficult to control the process precisely and to keep the coating molten at very low spray rates. Small-diameter pump tubing lessens the chance of hardening of the coating by increasing velocity at the same mass delivery rate. Particles less than 100 μm can be coated using the powder coater design, however, agglomeration potential increases with decreasing particle size.

Use of Optimization Techniques in Formulation

Response surface methodology has proven to be a useful technique in the development of pharmaceutical processes and formulations (11–15). Several fluid bed processes have been evaluated using these techniques (16,17), but to our knowledge they have not been used in the characterization of a hot-melt fluid bed coating process. The basic components of response surface methodology, first developed by Box and Wilson (18), include experimental design, regression analysis, and optimization algorithms. These are used to investigate the empirical relationship between one or more measured responses and a number of independent variables. The ultimate goal of these techniques is to obtain an optimal product or process. The specifics of the techniques are well described in the literature (19) and are not reviewed here. In this study, process optimization techniques were applied to a fluid bed hot-melt coating process using a fine granulate prepared by wet granulation.

MATERIALS AND METHODS

Properties of Materials

A sugar-based granulation was coated with partially hydrogenated cottonseed oil (Durkee 07 Stearine, Durkee Industrial Foods) in a Glatt GPCG-5 fluid bed unit by hot-melt top-spray techniques throughout this work. The partial saturation of the fatty acid chains of the triglyceride hardens this wax to a melting point of approximately 64°C. The ester linkages are primarily stearic acid (C-18) or palmitic acid (C-16) in length. This coating wax has a bland odor and virtually no taste, is approved as a food grade material, and is slightly yellow in color. Lot number J7166F was used throughout the study. It had a melting range of 64–67°C by differential scanning calorimetry (Perkin–Elmer DSC-7) with an enthalpy of fusion of 169 J/g. It is quite hydrophobic, showing a contact angle of 108.4° with water under 100%

relative humidity (Rame-Hart goniometer, $n = 17$, SD = 1.5°). The viscosity of molten partially hydrogenated cottonseed oil decreases gradually from 22 to 6 cps over the temperature range of 60–130°C (Brookfield LVTVD-II digital viscometer).

The granulation for the coating studies was an aqueous granulation of a hydrophobic nonionic drug (18% by weight) and powdered sugar made in a Fielder PMA 65 liter granulator (T. K. Fielder Ltd.). Lot-to-lot differences were eliminated as a process variable by preblending sufficient granulation for all batches in the study. The granulation was screened (Russell-Finex Sieve), and only those granules under 100 mesh (150 μm) were used in coating studies.

Description of the Coating Process

Uncoated granules were fluidized with an air volume of 220 m^3/hr, which allowed good fluidization patterns throughout the coating run. A nylon/carbon filament exhaust filter (PA/CF 9754, 3 to 10-μm pore size, Glatt Air Techniques, Ramsey, NJ) was used to prevent loss of the fine particles through the expansion chamber, and the bowl was lined with Polyester filter cloth (50-μm pore size, Glatt Air Techniques, Ramsey, NJ) to keep the granules from falling through the bottom mesh screen. The nozzle and wand were wrapped fully with insulating tape and placed in the bottom position in the expansion chamber to spray onto the densest portion of the bed. A Schlick two-fluid nozzle with a port size of 0.8 mm and an air dome setting of 3 × 360° provided good spray patterns with molten wax at all atomization pressures in the study. Atomization air was heated by passing the line through an oil bath and kept at temperatures near that of the molten wax. Figure 2 illustrates the configuration of the insulated nozzle and atomization air lines with respect to the melt vessel and fluid bed for this study. The filter was shaken in alternate halves at 15-sec intervals for 3 sec without interrupting fluidization or spraying. Batch sizes of 6 kg (uncoated) were initially provided with 60°C inlet air and adjusted from that point to maintain product bed temperatures just below the melting point of the wax throughout the coating phase. Molten wax was maintained at constant temperature on a hot plate and its application rate was measured by weight loss on a digital electronic balance (Sartorius top-loading). Coating was applied to 30% by weight (1.8 kg), and the coated particles were allowed to cool to 40°C before halting fluidization. Cooling was accomplished by turning off the inlet air heater and bypassing the atomization air heater.

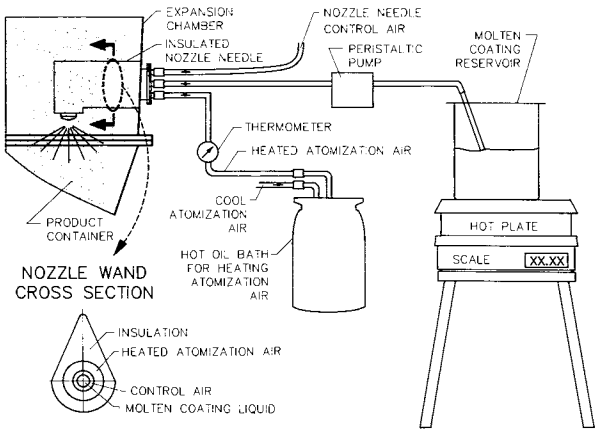

Fig. 2. Configuration of coating and atomization air lines for hot-melt coating, showing the relationship of heated air relative to the molten liquid in the insulated nozzle wand.

Experimental Design

Preliminary coating trials and previous experience by the authors had shown that the dominant variables affecting hot-melt coating processes are the product bed temperature during spray, the temperature of the molten wax, the atomization air temperature, the atomization air pressure, and the coating application or spray rate. Other variables of importance such as batch size, fluidization velocity, nozzle port size, and percentage coating were fixed at predetermined levels (detailed in the preceding paragraph) based on the initial trials. Product bed temperature was optimized for this particular wax and held constant (54°C) for the process optimization trials. Table I shows the levels used for each variable studied, including atomization air pressure, temperature, and spray rate. The temperatures of the molten wax and of the atomization air were studied as one confounded variable; that is, they were varied in concert to the levels indicated. Each variable was studied at low (−1), midpoint (0), and high (+1) levels that were equally spaced intervals which bracketed the expected region of optimum coating performance. The coded variable is used to preserve orthogonality and permit direct comparison of the magnitudes of the regression coefficients. A modified central composite design (20) was used for the study (Table I). The design consists of a full factorial portion (runs 1–8, Table I), centerpoint replicates (runs 9–12), Table I), and additional face-centered star points (runs 13–14, Table I) for the atomization air pressure. Preliminary experiments indicated that the atomization air pressure could cause curvature in the response surface,

Table I. Modified Central Composite Design for Three Variables

Coating run No.	Variable level		
	X_1[a]	X_2[b]	X_3[c]
1	−1	−1	+1
2	−1	−1	−1
3	−1	+1	+1
4	−1	+1	−1
5	+1	−1	+1
6	+1	−1	−1
7	+1	+1	+1
8	+1	+1	−1
9	0	0	0
10	0	0	0
11	0	0	0
12	0	0	0
13	0	0	+1
14	0	0	−1

[a] Temperature of molten wax and atomization air (80, 100, 120°C).
[b] Spray rate for wax coating (30, 45, 60 g/min).
[c] Pressure of atomization air (3, 4, 5 bar).

while the remaining variables had essentially linear effects. Four centerpoint replicates were performed to obtain an estimate of the experimental error and, hence, the relative significance of the variable effects. Second-order regression models were developed for the various responses in the form shown below:

$$Y_i = b_0 + b_1X_1 + b_2X_2 + b_3X_3 + b_{12}X_1X_2 + b_{13}X_1X_3 + b_{23}X_2X_3 + b_{123}X_1X_2X_3 + b_{33}X_3X_3 \quad (1)$$

where Y_i is the specific response being fitted, b_i is the regression coefficient, and X_i is the coded level of the independent variable. Regression analysis, contour plotting, and statistical optimization were performed on a commercially available personal computer-based software package called XSTAT (21). The coating trials were performed in random order over a period of 1 week at the Glatt testing facilities in Binzen, West Germany.

Responses and Measurement Techniques

Representative composite samples were taken of each run after coating and stored in amber glass bottles. The samples were subjected to various physical and chemical tests to evaluate the properties of the product and quantify the effect of process parameters on each response. Scanning electron microscopy (SEM) was used to evaluate the coating uniformity and surface morphology. Samples were coated with 200–300 Å of gold on a carbon-painted surface (Hummer VII coater, Anatech Ltd.) and evaluated at three magnifications on an ISI-DS 130 scanning electron microscope (International Scientific Instruments). Each batch was viewed as a population, a single particle, and a surface closeup, with care taken to choose an average particle in each case after observing many particles.

Ten samples from various portions of the container were assayed by HPLC for drug content (using hexane to extract the drug from the coating). The mean weight/weight percentage drug was used as the assay value for each batch, and the percentage relative standard deviation as a measure of uniformity. Dissolution rates in 0.1 *N* HCl and pH 7.5 phosphate buffer were measured on a flow-through system (Hewlett-Packard 8451A with dissolution software). The USP paddle method (at 100 rpm) and 900 ml of 37°C dissolution medium were used. Samples containing known amounts of drug (based on the assays) were shaken with simple syrup USP until uniformly suspended, and a known volume was added to the medium by syringe. The percentage dissolved, as compared to a reference solution of drug, was followed for 1 hr by ultraviolet detection.

The bulk density of each batch was measured by pouring coated granulation through a 1-cm orifice funnel into a graduated cylinder, and recording weight and volume occupied to calculate density (g/cm^3). Tapped density was calculated from the volume decrease following 1000 taps on an automated tap density machine (Vanderkamp). The means of three determinations per coating run were combined to arrive at a measure of powder flowability, the percentage compressibility proposed by Carr (22):

$$\% \text{ compressibility} = 100\ (\rho_t - \rho_0)/\rho_t \quad (2)$$

where ρ_t is the tapped density and ρ_0 is the bulk density. The smaller the percentage compressibility, the better the powder flowability. The mean particle size was determined by sieve analysis using one 100-g sample per coating run and six screens (having 250-, 180-, 150-, 125-, 106-, and 75-μm openings). These were shaken for 10 min on an automatic shaker (Ro-Tap) and the percentage weight in each size class was recorded. A software program based on the algebraic method of Motzi and Anderson (23) was used to calculate the mean particle size.

RESULTS AND DISCUSSION

Physical Properties of Coated Material

Preliminary experiments were performed to obtain an optimal product bed temperature. Bed temperatures were measured by a probe which sampled the moving bed approximately halfway from the product container bottom mesh. The maximum temperature which did not show agglomeration problems was desired, in order to minimize coat defects and achieve uniform wax distribution on the surface. Trials were performed using midpoint conditions for all other variables and 50, 54, and 58°C bed temperatures (based on the wax melting temperature). The 58°C sample showed extensive particle size growth, a wet sticky bed, and a rough surface appearance under SEM. This temperature approached the wax fusion temperature too closely and resulted in solidification times that were too long, causing "wet" particle–particle collisions which disrupted the coating before hardening. The 50 and 54°C samples showed uniform smooth coated surfaces; therefore 54°C was set as the product bed temperature. This could be maintained within ±1°C by adjusting the inlet air temperature throughout the run. Process times varied from 30 min (high spray rate) to 60 min (low spray rate) during the design trials. Trials using high spray rates exhibited heavier beds and appeared much wetter near the conclusion of the run. Electrostatic interactions caused the granules to stick to the expansion chamber initially, but as coating was applied, fluidization became regular and vig-

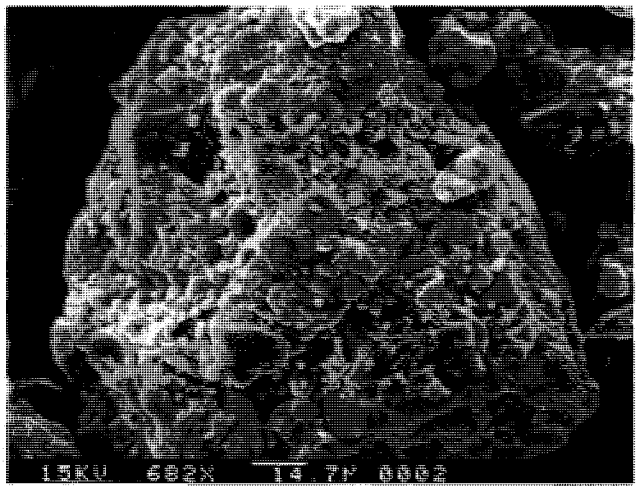

Fig. 3. Scanning electron micrograph of uncoated granulation particle. 682× magnification; reduced 70% for reproduction.

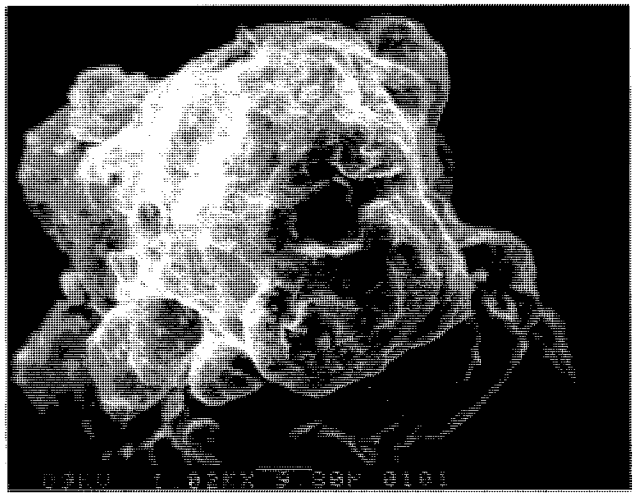

Fig. 4. Scanning electron micrograph of wax-coated granule. Coating run 13 at 1020× magnification; reduced 70% for reproduction.

orous. Yields varied from 99 down to 85%, and all of the material which did not stick to the walls or nozzle was used in the evaluations without further sizing.

Figure 3 shows an SEM of an average granule prior to coating, and Fig. 4 shows a wax-coated granule (30% coating by weight) from coating run 13 (midpoint wax/atomization temperature, midpoint spray rate, and high atomization air pressure). All SEMs taken were similar in surface appearance; no obvious morphological changes resulted from varying any of the parameters, although some runs had larger particles on the average. Different shapes and sizes of individual particles masked the effects of the processing conditions during manufacture. Figure 5 shows a surface closeup (run 6, high temperature, low spray rate, low atomization pressure) that is typical of the coated granules; there are smooth rounded corners that mask the roughness seen in uncoated granules and patterns that suggest that the wax spreads on the surface prior to hardening.

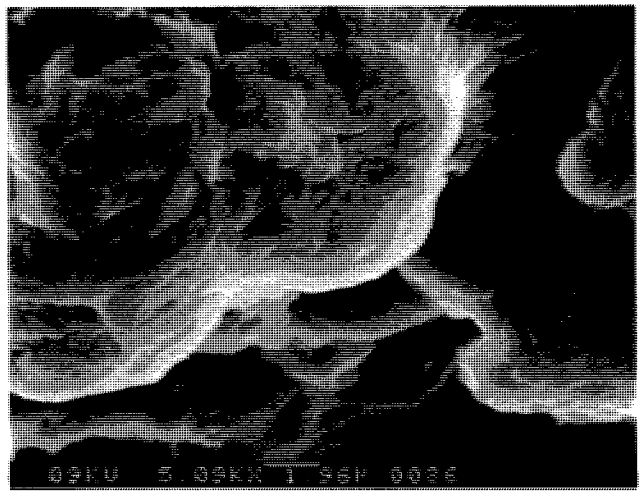

Fig. 5. Closeup SEM of surface morphology of wax-coated particle. Coating run 6 at 5090× magnification; reduced 70% for reproduction.

Table II summarizes the results for the quantitative responses measured on a representative sample for each coating run. The assay value (% drug) of each coated granule run was within the range expected upon applying a 30% coating to uncoated granules consisting of 17–18% drug. Reasonable uniformities were obtained; these were only slightly higher than the 0.8% RSD obtained for the uncoated granulation. The high value for run 3 may be real or may be a consequence of the small number of replicates (10 samples assayed). The bulk density decreased slightly for all coating runs (0.69 g/cm^3 for the uncoated sample), but the tapped densities varied in behavior depending on the coating conditions (uncoated value, 0.76 g/cm^3). Mean particle size varied considerably, but always increased (as expected) from the size of the uncoated material (mean size, 77 μm). The atomization air pressure strongly affected the particle size, such that this can be seen even before statistical analysis. Those runs with large mean particle sizes were performed at low atomization air pressures and exhibited agglomeration under the light microscope. The flowability measures generally increased (from the uncoated value of 9.1%), indicating a reduction in powder flowability upon wax coating application, but all values are still in the range defined by Carr as "good" flow (22). Dissolution results were essentially independent of the medium pH; this is readily apparent in Fig. 6, which plots the dissolution results from run 3 in both 0.1 *N* HCl and pH 7.5 phosphate buffer. This is as expected for a system containing a nonionic drug and a neutral triglyceride ester coating, both of which are nonionizable throughout this pH range. The dissolution data in Table II and Fig. 6 represent the mean of three determinations for each run in each medium. The standard deviation of these determinations was typically 1–2%.

Fitted Regression Models

Table III summarizes the results of the regression analysis after fitting a second-order model to each response [Eq. (1)]. The correlation coefficients, *F* ratios, and model significance level were acceptable in all cases except for the bulk density (Y_3) and flow (Y_6) responses. The variability in these data could not be accounted for by the processing parameters using this model. The percentage drug by assay (Y_1) and content uniformity (Y_2) were statistically affected by the process parameters, but the response range covered in the inference space was not practically relevant. All lots made under any of the combinations of variables employed had acceptable values of bulk density, flow, potency, and uniformity (see Table II); thus, they were not used in determining optimum coating parameters. Tapped density, particle size, and the dissolution responses were changed significantly by altering the coating parameters and were considered the relevant response variables for the study. As indicated by the magnitude of the regression coefficients in Table III, the atomization air pressure (X_3) had the greatest effect on the relevant responses. As the atomization air pressure is increased, a reduction in mean particle size occurs, whereas the tapped density and percentage drug dissolved are increased. The spray rate of the molten wax (X_2) also significantly affects the relevant responses (Table III). An

Table II. Values of the Measured Responses

Run No.	Y_1, percentage drug	Y_2, content uniformity	Y_3/Y_4, density (g/cm^3), bulk/tapped	Y_5, particle size (mean μm)	Y_6, flow (% compress.)	Y_7/Y_8, dissolution (%/hr), acid/neutral pH
1	12.8	1.35	0.64/0.75	103.6	12.3	57.3/64.0
2	13.3	1.01	0.62/0.72	113.8	13.8	56.6/54.8
3	12.8	3.31	0.65/0.77	100.5	15.3	59.9/60.0
4	13.5	0.98	0.61/0.68	139.4	10.9	25.2/25.7
5	12.6	1.62	0.67/0.78	106.8	13.8	74.1/70.1
6	13.2	1.19	0.64/0.70	124.3	8.5	37.6/40.8
7	13.2	1.30	0.63/0.72	114.6	12.1	39.3/41.1
8	13.2	1.04	0.61/0.70	127.8	12.7	41.1/43.6
9	13.7	1.24	0.64/0.75	94.9	12.8	60.5/59.9
10	13.4	1.86	0.66/0.74	99.2	11.3	57.2/58.0
11	13.3	1.39	0.64/0.73	114.4	12.0	47.6/51.4
12	13.4	1.01	0.60/0.72	107.8	16.3	40.8/43.2
13	13.2	1.30	0.65/0.75	103.9	12.1	47.8/47.0
14	13.2	1.30	0.60/0.70	130.5	15.2	32.8/34.6

increase in spray rate generally results in a larger mean particle size and lower values for tapped density and percentage dissolution of the coated material. This would be expected, as increasing spray rates typically caused a change in atomization patterns at constant pressures. Within the inference space of the design, the temperature of the molten wax/atomization air (X_1) had little effect on the relevant responses (Table III). Three-way interaction exists between the process variables (b_{123}) and significant curvature in the response surface is evident (b_{33}) for the tapped density and mean particle size responses.

Optimization of the Coating Process

The optimum product was defined as one having high dissolution and small particle size (no agglomeration) and acceptable values of the less critical parameters (potency, uniformity, flowability, and bulk/tapped density). The percentage drug dissolved in 0.1 *N* HCl was chosen as the objective function and was maximized at a wax/atomization temperature of 120°C, a spray rate of 30 g/min, and an atomization air pressure of 5.0 bar, using the simplex technique incorporated in the XSTAT software package (21). This also corresponds to the maximum tapped density and results in a particle size very close to the minimum. SEM had shown that the coating was complete in all cases, and potency/uniformity results were in the expected range. Better flowability would be desirable but is not possible at any combination of these variables in this region (or with particles this small). These conditions were chosen as optimal for this process on this machine. Since these are on the corner of the design, consideration was given to extending the region of study in that direction, but this was not considered feasible. Higher molten wax temperatures would not have much of an effect and posed safety issues. Atomization air pressure is equipment-limited (to about 6 bar), but operation at the machine's limit would reduce reproducibility and restrict fine-tuning in later work. Finally, slower spray rates would make the process impractical in a production environment.

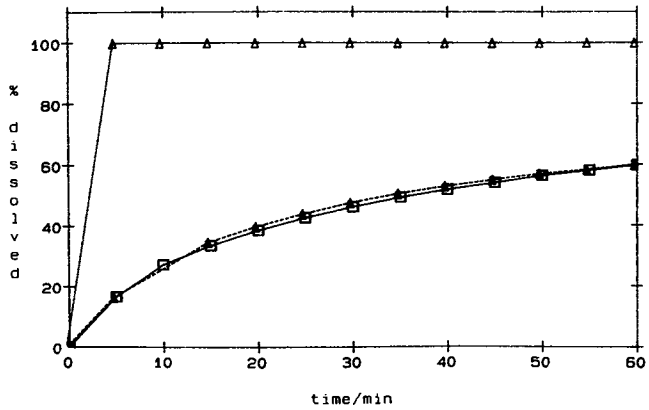

Fig. 6. Dissolution data by USP paddle method at 37°C and 100 rpm. (△) Uncoated granulation in both 0.1 *N* HCl and pH 7.5 phosphate buffer; (▲) wax-coated granulation (coating run 3) in pH 7.5 phosphate buffer; (□)wax-coated granulation (coating run 3) in 0.1 *N* HCl.

Figures 7–9 depict the effects of the major variables (spray rate and atomization air pressure) on tapped density, dissolution in 0.1 *N* HCl, and mean particle size while wax/atomization air temperature is fixed at the high level (the optimum level which maximizes dissolution). The fitted regression results are shown as both three-dimensional graphs (upper) and contour plots with constant levels indicated (lower). Response surfaces and contour plots were generated from the full regression model. The upper left corner of each contour plot represents the coating conditions chosen as optimum. Movement in most directions results in lower dissolution rates, lower densities, and larger mean particle sizes. Significant interaction between the plotted variables is especially evident for tapped density (Fig. 7) and percentage drug dissolved (Fig. 9). Significant curvature in the response surface with changes in atomization air pressure is readily apparent for the mean particle size (Fig. 8).

The optimum product bed temperature (54°C) and the wax/atomization air temperature (120°C) are a function primarily of the coating wax and would be expected to be the

Table III. Summary of Regression Results for the Measured Responses

Coefficient	Regression coefficient value for response Y_i[a]							
	Y_1	Y_2	Y_3	Y_4	Y_5	Y_6	Y_7	Y_8
b_0	13.45	1.38	0.635	0.735	104.1	13.1	51.5	53.1
b_1	X	−0.19	X	X	X	X	X	X
b_2	0.10	0.18	X	−0.010	4.23	X	−7.5	−7.4
b_3	−0.18	0.34	0.016	0.027	−10.64	X	8.5	8.3
b_{12}	X	−0.30	X	X	X	X	X	X
b_{13}	X	−0.25	X	X	X	X	X	X
b_{23}	X	0.23	X	X	X	X	X	X
b_{123}	0.10	−0.27	X	−0.015	4.13	X	−9.0	−7.1
b_{33}	−0.35	X	X	−0.009	12.44	−1.6	X	X
r[b]	0.908	0.909	0.804	0.973	0.944	0.706	0.916	0.916
F[c]	2.95	3.39	1.14	10.92	5.10	0.62	3.25	3.26
p[d]	0.135	0.110	0.458	0.022	0.060	0.734	0.117	0.117

[a] X indicates that the regression coefficient was not significant at $\alpha = 0.25$.
[b] Multiple correlation coefficient.
[c] Mean square regression/mean square residual.
[d] The attained significance level for the model.

same in any size fluid bed. Spray rate and atomization pressure are also functions of nozzle sizes, batch sizes, and heating/fluidization capacity, so the absolute settings will change by machine size. However, in subsequent studies, the trends remained the same; adjustment to higher pressures and slower spray rates favored less agglomeration and improved dissolution. In a Glatt GPCG-3 machine using batch sizes half that of this study, a spray rate of 15 g/min and a pressure of 4.0 bar produced the same results as the optimum conditions in the GPCG-5 of this work. Limited experience at the 100-kg batch size showed again that spray rate and particle size were directly related, and atomization air pressure and particle size were inversely related, with atomization air pressure being the dominant variable.

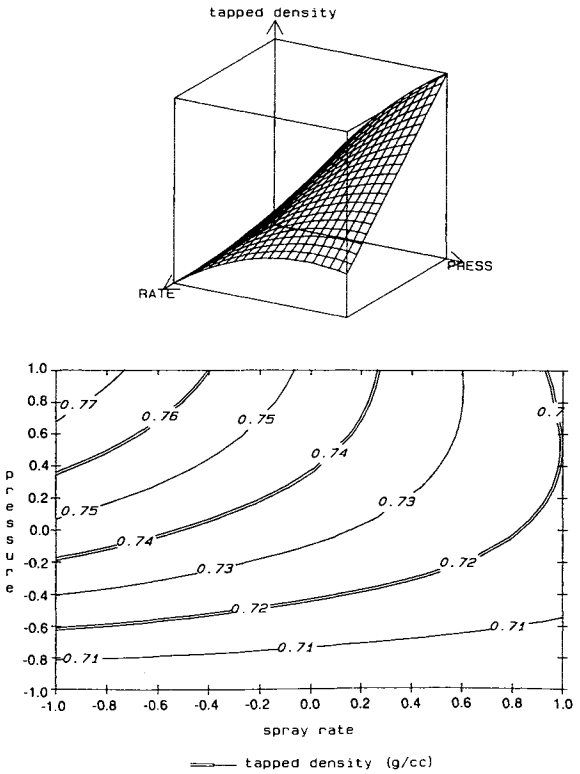

Fig. 7. Contour plot and three-dimensional (3-D) graph showing the variation of tapped density (Y_4) with spray rate (X_2) and atomization air pressure (X_3) while temperature (X_1) is fixed at the high level (120°C).

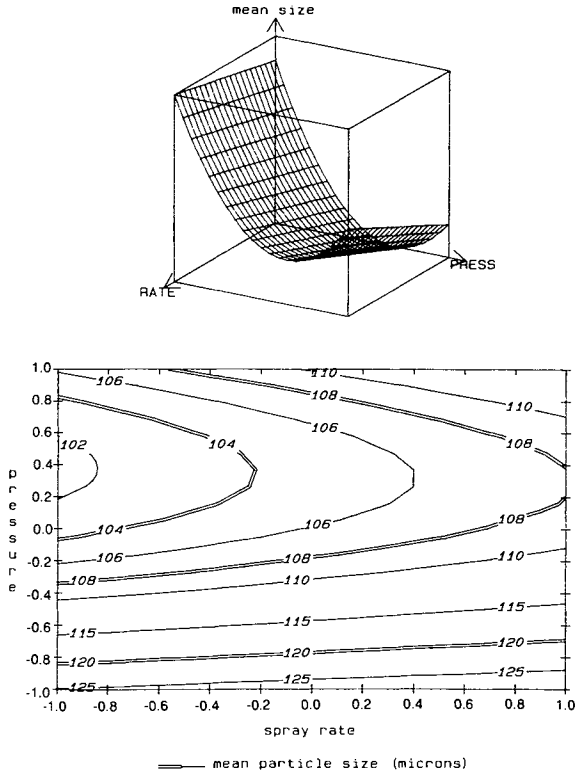

Fig. 8. Contour plot and 3-D graph showing the variation of mean particle size by sieve analysis (Y_5) with spray rate (X_2) and atomization air pressure (X_3) while temperature (X_1) is fixed at the high level (120°C).

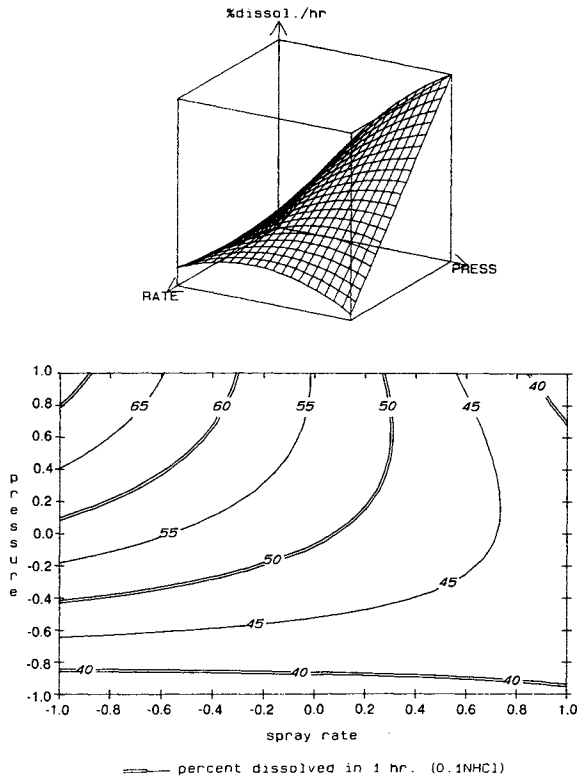

Fig. 9. Contour plot and 3-D graph showing the variation of dissolution in 0.1 *N* HCl (Y_7) with spray rate (X_2) and atomization air pressure (X_3) while temperature is fixed at the high level (120°C).

ACKNOWLEDGMENTS

The authors wish to acknowledge Mr. J. O. Mullis (Glaxo Inc., Analytical Chemistry Department) for taking the photomicrographs and Mr. A. W. Wood (Glaxo Inc., Pharmaceutics Department) for examining the physical properties of the coating wax. We thank Mr. D. K. Wilbourne, Mr. C. P. Childers, and Mr. M. A. Rose (all of Glaxo Inc., Analytical Chemistry Department) for performing the potency assays. Mr. David Cooper assisted with the statistical analysis (Glaxo Inc. Management Information Services, Statistics).

REFERENCES

1. I. S. Hamid and C. H. Becker. *J. Pharm. Sci.* **59**:511–514 (1970).
2. A. G. Cusimano and C. H. Becker. *J. Pharm. Sci.* **57**:1104–1112 (1968).
3. P. M. John and C. H. Becker. *J. Pharm. Sci.* **57**:584–589 (1968).
4. S. Motycka and J. G. Nairn. *J. Pharm. Sci.* **67**:500–503 (1978).
5. S. P. Patel and C. I. Jarowski. *J. Pharm. Sci.* **64**:869–872 (1975).
6. C. I. Igwilo and N. Pilpel. *Int. J. Pharm.* **15**:73–85 (1983).
7. C. I. Irono and N. Pilpel. *J. Pharm. Pharmacol.* **34**:480–485 (1982).
8. C. Igwilo and N. Pilpel. *J. Pharm. Pharmacol.* **39**:301–302 (1987).
9. E. Mathiowitz and R. Langer. *J. Control. Release* **5**:13–22 (1987).
10. C. R. Kowarski and F. Tiano. *Pharm. Acta Helv.* **50**:310–312 (1975).
11. D. E. Fonner, Jr., J. R. Buck, and G. S. Banker. *J. Pharm. Sci.* **59**:1587–1596 (1970).
12. J. B. Schwartz, J. R. Flamholz, and R. H. Press. *J. Pharm. Sci.* **62**:1165–1170 (1973).
13. K. Takayama and T. Nagai. *Chem. Pharm. Bull.* **37**:160–167 (1989).
14. R. M. Franz, J. A. Sytsma, B. P. Smith, and L. J. Lucisano. *J. Control. Release* **5**:159–172 (1987).
15. R. M. Franz, J. E. Browne, and A. R. Lewis. In H. A. Lieberman, M. M. Rieger, and G. S. Banker (eds.), *Pharmaceutical Dosage Forms: Disperse Systems*, Marcel Dekker, New York, 1988, pp. 427–514.
16. J. Spitael and R. Kinget. *Int. Conf. Powder Technol. Pharm.* **1**:1–11 (1978).
17. V. I. Gorodnichev, H. M. El-Banna, and B. V. Andreev. *Pharmazie* **36**:270–273 (1981).
18. G. E. P. Box and K. B. Wilson. *J. R. Stat. Soc.* **13**:1–45 (1951).
19. G. E. P. Box and N. R. Draper. *Empirical Model Building and Response Surfaces*, Wiley, New York, 1987.
20. R. H. Myers. *Response Surface Methodology*, Library of Congress Catalog Card No. 71-125611, 1976.
21. J. S. Murray. *X-Stat—Statistical Experiment Design/Data Analysis/Nonlinear Optimization*, Wiley, New York, 1984.
22. R. L. Carr. *Br. Chem. Eng.* **15**:1541 (1970).
23. J. J. Motzi and N. R. Anderson. *Drug Dev. Ind. Pharm.* **10**:225–239 (1984).